Talanta 119 (2014) 151–155

Contents lists available at ScienceDirect

Talanta

journal homepage: www.elsevier.com/locate/talanta

Characterization of plasma-enhanced teflon AF for sensing benzene, toluene, and xylenes in water with near-IR surface plasmon resonance

Tim A. Erickson [a,*], Rajvir Nijjar [b], Matt J. Kipper [b], Kevin L. Lear [a,*]

[a] Department of Electrical and Computer Engineering, Colorado State University, Colorado 80523-1373, USA
[b] Department of Chemical and Biological Engineering, Colorado State University, Colorado 80523-1370, USA

ARTICLE INFO

Article history:
Received in revised form
17 October 2013
Accepted 18 October 2013
Available online 24 October 2013

Keywords:
Aromatic hydrocarbon sensing
BTEX
Teflon AF
Surface plasmon resonance
Water quality
Environmental monitoring

ABSTRACT

Near-IR surface plasmon resonance is used to characterize Teflon AF films for refractive index-based detection of the aromatic hydrocarbon contaminants benzene, toluene, and xylenes in water. The technique requires no sample preparation, and film sensitivity is found to be enhanced by oxygen plasma etching. A diffusion equation model is used to extract the diffusion and partition coefficients, which indicate film enrichment factors exceeding two orders of magnitude, permitting a limit of detection of 183, 105 and 55 ppb for benzene, toluene, and xylenes, respectively. The effect of other potential interfering contaminants is quantified.

1. Introduction

Contamination of water supplies by aromatic hydrocarbons, such as benzene, toluene, and xylene (BTX) can pose a significant threat to human health [1–3]. Recent contamination incidents include BTX contamination of the aquifer near Pavillion, Wyoming indicated to be caused by hydraulic fracturing [4] as well as benzene contamination of Parachute Creek in Colorado caused by a leaking pipeline [5]. The goal of detecting and localizing contamination events in real time motivates the development of low-cost, portable sensing systems.

The current gold standard for BTX detection in water is head-space trap sampling of suspected water samples using tandem gas chromatography/mass spectrometry [6]. While such systems can provide exquisite sensitivity (0.002 ppb) they are bulky and require significant sample preparation, and therefore cannot be permanently embedded in the vicinity of a pipeline or within a water tap to continuously monitor water quality. In contrast, dielectric-based sensors, such as DMFETs [7] and refractive index-based sensors such as the LEAC optoelectronic chip [8] are very compact ($\sim$1 cm^2) and require no sample preparation for the proposed sensing mechanism, while offering cost advantages due to system simplification. All refractive index-based sensors require a functionalized sensing element, which captures the analyte of interest.

Teflon AF is an amorphous fluoropolymer, which can readily be spin-coated onto sensors, forming a chemically stable, hydrophobic film [9]. In this work, we demonstrate the utility of oxygen plasma etched Teflon AF for refractive-index based detection of aromatic hydrocarbon contaminants in water. The diffusion and partition coefficients of BTX contaminants in Teflon AF 1600 films are characterized using near-IR surface plasmon resonance (SPR). Due to its low refractive index (n=1.31) [9], excellent stability in a variety of chemical environments [10], extreme hydrophobicity [11], and high fractional free volume [12], Teflon AF films are well-suited for refractive index-based detection of BTX contaminants, which are found to concentrate in the films. As BTX have a significantly higher index [13] ($n\sim$1.48 at 1040 nm), partitioning into Teflon AF leads to a measurable increase in the film's refractive index. A limit of detection and sensitivity (Δn/ppm) is determined for each BTX analyte. Interference from temperature drift and other contaminants with a wide range of octanol–water partition coefficients [14], which can also permeate into the film, is quantified.

Teflon AF films have previously been characterized for refractive index-based detection of BTX vapors in air [15], while others have investigated the pervaporation and sorption properties of pure BTX samples [10] and the transport dynamics of BTX in chloroform solutions [16]. Edwards et al., have previously employed Teflon films for sensing BTX compounds in water [17], but the diffusion and

* Corresponding authors. Tel.: +1 970 491 6158.
E-mail addresses: timaerickson@gmail.com (T.A. Erickson), Kevin.Lear@colostate.edu (K.L. Lear).

0039-9140/$ - see front matter © 2013 Elsevier B.V. All rights reserved.
http://dx.doi.org/10.1016/j.talanta.2013.10.038

partition coefficients of BTX were not investigated; the films were not plasma etched, and interference from other non-BTX solutes was not quantitatively characterized. As any aqueous environment may contain a number of solutes, including BTX, it is important to quantify the matrix effects of potential interfering contaminants.

2. Experimental

2.1. Sample preparation

For SPR experiments, a separate Teflon /gold/SF-10 glass SPR sensing substrate was used for each analyte. Sensing substrates were prepared by first thermally evaporating a 2.5 nm Cr adhesion layer onto cleaned SF-10 glass slides [18], followed by deposition of 47.5 nm of Au at a rate of 0.1 nm/s. After metal evaporation, a 2950 nm Teflon AF 1600 sensing layer was deposited on top of the Au layer. As Teflon AF does not readily adhere to Au, a 1:20 dilution of 1H, 1H, 2H, 2H-Perfluorodecyltriethoxysilane (97%) with methanol was used as an adhesion promoter by spin-coating onto the gold layer at 800 RPM for 30 s followed by a 10 min hot plate bake at 120 °C. After application of the adhesion promoter, three successive layers of Teflon AF 1600-6 (Dupont) were applied to the substrate. The Teflon AF polymer at 6% concentration in a solution of Fluorinert FC-40 was spin-coated onto the substrate at 1000 RPM for 1 min and cured by successive 5 min hot plate bakes at 70 °C, 100 °C, 120 °C, 160 °C, 200 °C, 260 °C. After cooling, all sensing samples were oxygen plasma etched for 10 s using a MicroTechnics RIE at a flow rate of 50 sccm and power of 50 W after each layer was applied. Plasma etching was found to increase the water contact angle from 120° to 132°. (Control samples were not etched after the third Teflon layer had been cured.) This process yielded a Teflon layer of 2950 ± 50 nm, as measured by white light spectrometry and profilometry. The adhesion promoter is only applied once, as the plasma etching is used to bind multiple layers of Teflon films. Furthermore, plasma etching after the last layer serves to increase both hydrophobicity and sample surface roughness [19].

Solutions of high-purity benzene, toluene, and a mixture of the three xylene isomers were prepared using deionized water at concentrations of 1 ppm, 3 ppm, 10 ppm, and 30 ppm. In order to analyze the film's specificity and check for interference from other solutes, samples of *n*-hexane (30 ppm), dichloromethane (300 ppm), diethyl ether (3000 ppm), acetone (3000 ppm), methanol (3000 ppm), ethylene glycol (3000 ppm) and municipal tap water (Fort Collins, CO) were also prepared. To avoid temperature-related effects, all samples, consisting of 1 L of fluid, were allowed to equilibrate to room temperature (22 °C) and were repeatedly agitated to ensure a homogenous mixture.

2.2. SPR Measurements

A Nicolet SPR 100 connected to a Nicolet 8700 FT-IR spectrometer was used to acquire SPR data. The apparatus employs a broadband near-IR source to excite surface plasmons in the Kretschmann configuration by using an SF-10 prism and index matching fluid. The incident near-IR light is introduced at a fixed angle of incidence, and the wavelength of the light is modulated by the interferometer in the FT-IR spectrometer. Sample solutions were introduced into the SPR flow cell using a peristaltic pump and fluid was drawn from the middle of the sample reservoir. SPR spectra were acquired at a rate of 8 Hz and 32 spectra were averaged over 4 s to improve the signal-to-noise ratio. A center-of-gravity weighting function was used to estimate the absorption peak λ_o. All experiments were initialized with the SPR absorption peak at approximately 1040 nm. Oxygen plasma etched Teflon sensing substrates were used for all experiments, except for comparison experiments between etched and non-etched films, which were carried out for the BTX solutes at a concentration of 30 ppm.

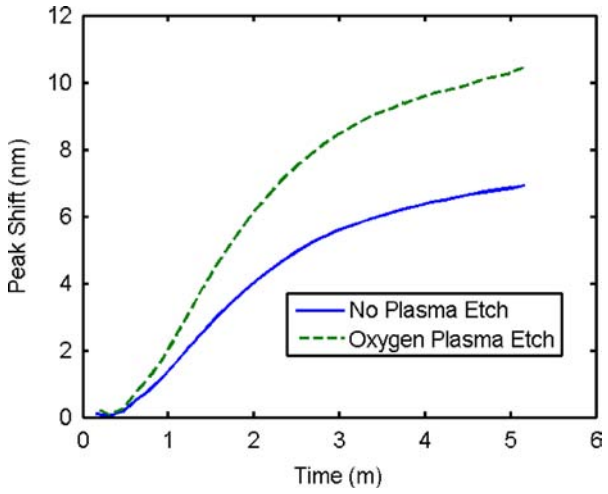

Fig. 1. Effect of oxygen plasma etching on Teflon AF film sensitivity to benzene (30 ppm).

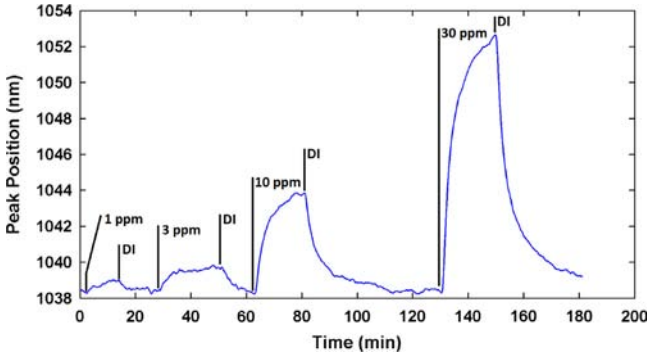

Fig. 2. SPR time trace vs. peak position for benzene. The times at which deionized water (DI) and different concentrations of benzene (1, 3, 10, and 30 ppm) were introduced into the flow cell are annotated on the plot. The first 1 ppm concentration of benzene was added at 2 min to the flow cell which had previously been filled with DI water.

3. Results and discussion

3.1. Effect of oxygen plasma etching

Oxygen plasma etching renders the Teflon AF surface superhydrophobic [19]. In Fig. 1, the SPR peak shift vs. time is plotted for oxygen plasma etched and non-etched films exposed to a 30 ppm solution of benzene. As indicated by Fig. 1, plasma etching enhances analyte solute uptake, leading to an increased peak shift. In triplicate measurements, the increased surface hydrophobicity was found to increase the film's sensitivity to benzene, toluene, and xylenes at concentrations of 30 ppm by $50 \pm 3\%$, $53 \pm 2\%$, and $58 \pm 4\%$, respectively, during the 5 min sample period. For all remaining experiments, only oxygen plasma enhanced films were used.

3.2. SPR data for calculating the LOD, diffusion and partition coefficients

A characteristic SPR peak position vs. time trace is shown in Fig. 2 for benzene at concentrations of 1, 3, 10 and 30 ppm. DI Water is pumped through the flow cell after each benzene run in order to remove the diffused solute and bring the signal

back to baseline. While regeneration time increases with solute concentration, no significant hysteresis is observed. Notably, the 1 ppm concentration can be readily distinguished from baseline, indicating a sub-ppm limit of detection.

An identical set of experiments was repeated for xylene and toluene, as well as n-hexane at a single concentration (30 ppm). The bulk index change of the film Δn_{bulk} can readily be determined by multiplying the shift in peak position by the SPR's measured responsivity. The responsivity of the SPR system was measured to be 1.14×10^4 nm/RIU by linear regression fitting ($r^2=0.998$) of sucrose solutions [20] at concentrations of 0, 0.25, 0.5, and 1% on a Teflon-free gold substrate.

3.3. Analytical extraction of diffusion and partition coefficients

The partition K and diffusion D coefficients were extracted by fitting the observed index change Δn_{bulk} in the Teflon film to a one-dimensional diffusion model, which is justified by the planar film geometry. For a concentration C (#/cm^3), diffusion direction z, and time t, the diffusion equation is given by:

$$\frac{dC}{dt}=D\frac{d^2C}{dz^2} \tag{1}$$

The initial concentration of solute in the film is taken to be zero. The boundary condition at the solution/film interface is set by assuming the contaminant concentration in the uppermost film layer ($z=z_{film}=2950$ nm) is immediately equilibrated [21], such that $C(z=z_{film}, t)=KC_o$, where C_o is the concentration of the solute in solution. A no-flux boundary condition ($dC/dz=0$) was used for the Teflon/Au interface at $z=0$. For these boundary conditions, the solution of the diffusion equation is given by [22],

$$C(z,t)=KC_o-\frac{4KC_o}{\pi}\sum_{n=0}^{\infty}\frac{(-1)^n}{2n+1}exp\left\{\frac{-D(2n+1)^2\pi^2t}{4{z_{film}}^2}\right\}\cos\left\{\frac{(2n+1)\pi z}{2z_{film}}\right\} \tag{2}$$

As a given solute permeates into the film, its concentration and hence the localized change in refractive index $\Delta n(z)$ are governed by the diffusion equation. Thus, the evanescent tail of the supported surface plasmon probes a varying range of concentrations, and further analysis is required to relate the observed peak shift to z-dependent concentration profile of the film.

At 1040 nm, gold has a complex dielectric function [23] of $-47.88+2.911i$. Assuming a refractive index of $n=1.31$ for the Teflon film [9], the evanescent field decay length [24] is approximately 656 nm. As such, the field probes a relatively thick region of the film in the z-direction and perturbation theory [24] is required to relate the measured value Δn_{bulk} to the localized refractive index change in the film $\Delta n(z)$ caused by analyte diffusion. For an evanescent field $E(z)=E_o exp(-\gamma z)$, where $\gamma=1/656$ nm, the measured effective bulk index change Δn_{bulk} is related to position-dependent index change $\Delta n(z)$ by:

$$\Delta n_{bulk}\approx\frac{\int_0^{z\_film}E(z)\Delta n(z)E(z)\,dz}{\int_0^{z\_film}E(z)E(z)\,dz}=\frac{\int_0^{z\_film}\Delta n(z)\exp(-2\gamma z)\,dz}{\int_0^{z\_film}\exp(-2\gamma z)\,dz} \tag{3}$$

As an approximation, the integral is only carried out to the edge of the film ($z\_film=2950$ nm), as 99.99% of the evanescent field intensity is located within the film.

In order to extract K and D from the diffusion model, Eq. (2) was calculated for a wide matrix of diffusion (D=2000:20:30,000) and partition coefficients (K=0:1:1,500) to yield $C(z,t)$ for each analyte in 4 s intervals over a range of 15 min. The localized refractive index change $\Delta n(z)$ was computed using the Lorentz-Lorenz relation [15] with $C(z)$, polarizability α_c and solute-free Teflon film index $n=1.31$. For the change in local index $\Delta n(z)$, the relation can expressed as,

$$\frac{(n+\Delta n(z))^2-1}{(n+\Delta n(z))^2+2}-\frac{n^2-1}{n^2+2}=\frac{1}{3\epsilon_o}C(z)\alpha_c \tag{4}$$

and numerically solved for $\Delta n(z)$. Polarizability of each analyte at 1040 nm was computed using Cauchy fits to the data in Ref. 13 and then applying the standard Lorentz-Lorenz relation [25]. After solving for $\Delta n(z)$ for each analyte, Eq. (3) is then used to relate $\Delta n(z)$ to the measured SPR bulk refractive index Δn_{bulk} as a function of time. Lastly, K and D are then extracted from the diffusion theory model, using a least-squares fitting algorithm, which minimizes the residual between the measured data (Δn_{bulk} vs. time) and the model over a 15 min interval. In the context of curve fitting, K and D are independent parameters, as D only affects the shape of the fitted curve, and K only affects the magnitude of the total signal, serving as a multiplicative constant. The data and fitted curves for 30 ppm solutions of xylene, toluene, benzene, and n-hexane are displayed in Fig. 3. As seen in Fig. 3, there is excellent agreement between the experimental data and diffusion model-based fit. 1 ppm, 3 ppm, and 10 ppm concentration of the aromatic hydrocarbons were analyzed in the same manner.

The extracted K and D for each concentration are provided in Table 1 along with maximum error bounds, indicated by brackets. The data indicate both K and D are relatively insensitive to concentration, but are highly sensitivity to analyte type, with the D decreasing with analyte size, and K increasing with analyte size. Based on the extracted diffusion constants, film thickness, and optical field profile, the approximately 15 min exposure time to each BTX analyte concentration allowed for the refractive index response at the Teflon/gold interface to reach 99%, 96% and 83% of the equilibrium values for benzene, toluene and xylene, respectively.

As a method to characterize measurement uncertainty, simulations were repeated for film thicknesses of 2900 and 3000 nm to account for variations in film thickness, yielding error bounds due to film thickness uncertainty δd_{film}. Measurement uncertainty due to fitting error δfit was computed as follows. Using a mean film height of 2,950 nm, K and D were then independently varied until the residual was double the minimum residual value, yielding error bounds related to curve fitting. Maximum error bounds for both K and D were then computed by taking the sum of δfit and δd_{film}.

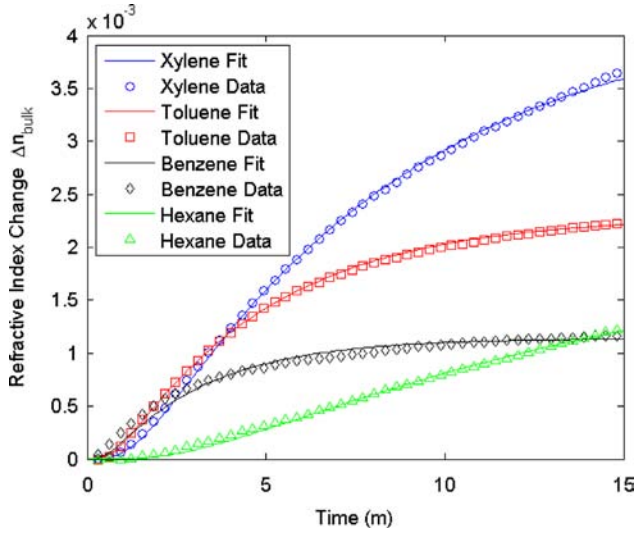

Fig. 3. Measured bulk refractive index change and model based fit for 30 ppm concentrations of xylene, toluene, benzene, and hexane.

Table 1
Calculated diffusion (D) and partition coefficients (K) for aromatic hydrocarbons in Teflon AF 1600.

Analyte	Concentration (ppm)	D (10^{-10} cm^2/s)	K ($C_{film}/C_{solution}$)
Benzene	30	2.06 [1.92 to 2.20]	258 [241 to 276]
	10	2.03 [1.86 to 2.31]	242 [230 to 254]
	3	2.01 [1.79 to 2.38]	235 [221 to 249]
	1	1.96 [1.61 to 2.50]	262 [233 to 291]
Toluene	30	1.37 [1.33 to 1.41]	451 [438 to 465]
	10	1.22 [1.14 to 1.31]	444 [423 to 464]
	3	1.12 [0.93 to 1.36]	432 [404 to 457]
	1	1.02 [0.84 to 1.43]	415 [380 to 460]
Xylenes	30	0.78 [0.76 to 0.80]	845 [824 to 862]
	10	0.75 [0.70 to 0.82]	832 [804 to 863]
	3	0.73 [0.66 to 0.82]	808 [736 to 868]
	1	0.71 [0.63 to 0.85]	788 [706 to 857]

3.4. Calculated film sensitivity and limit of detection

At the concentrations tested, both the diffusion and partition coefficient are relatively constant for each analyte. The small range ($<10\%$ deviation) of partition coefficient values indicate a linear sensitivity (Δn/ppm), as previously demonstrated for BTX vapor sensing experiments [15]. The film's refractive index sensitivity to each BTX contaminant at full equilibrium was determined by linear fitting ($r^2=0.97$) to be to be 4.1×10^{-5}/ppm, 7.1×10^{-5}/ppm, and 1.4×10^{-4}/ppm for benzene, toluene and xylenes, respectively.

The limit of detection (LOD) for each BTX analyte is calculated as follows. A 5-point moving average filter is first used to improve SNR. Δn_{bulk} was computed from the measured total peak shift $\Delta\lambda_o$ at 1 ppm, while the standard deviation $\delta\lambda_o$ was determined in DI water for 8 measurements (32 s) in the period before analyte introduction. Three times the standard deviation, per the IUPAC definition [26], was found to be 0.103 nm, corresponding to a refractive index resolution of $\Delta n=7.5\times10^{-6}$ RIU. Using this methodology, LODs for benzene, toluene, and the xylene mixture were found to be 183, 105, and 55 ppb, respectively. These LOD values are significantly lower than the values found for vapor measurements in air [15] due in large part to increased film sensitivity resulting from higher partition coefficients for BTX diffusing from an aqueous environment rather than air. It is important to note that temperature stability or a method to account for temperature fluctuations is essential to achieving accurate and precise measurement values. Temperature variation measurements from DI water show a combined film/SPR system response ($\Delta n/\Delta T$) of 1.4×10^{-5}/°C. No measureable difference in SPR signal was observed between DI water and municipal tap water equilibrated to the same temperature.

3.5. Sample matrix interference effects

In order to analyze the film's specificity and check for interference from other solutes, samples with a wide range of octanol-water partition coefficients [14] were also measured and analyzed. The film's sensitivity response (Δn/ppm) vs. octanol-water partition coefficient log(P_{ow}) is plotted in Fig. 4 for hexane (log(P_{ow})=4.0), xylene (log(P_{ow})=3.15), toluene (log(P_{ow})=2.73), benzene (log(P_{ow})=2.13), dichloromethane (log(P_{ow})=1.25), diethyl ether (log(P_{ow})=0.89), acetone (log(P_{ow})=−0.24), methanol (log(P_{ow})=−0.82), and ethylene glycol (log(P_{ow})=−1.36). As indicated by the logarithmic plot, there is a strong correlation between the Teflon-water partition coefficient and the octanol-water partition coefficients. A linear fitting of the data yields the equation: log(K)=0.659 log (P_{ow})+0.738 ($r^2=0.943$). Thus, the film shows an increasing selectivity toward increasingly hydrophobic contaminants.

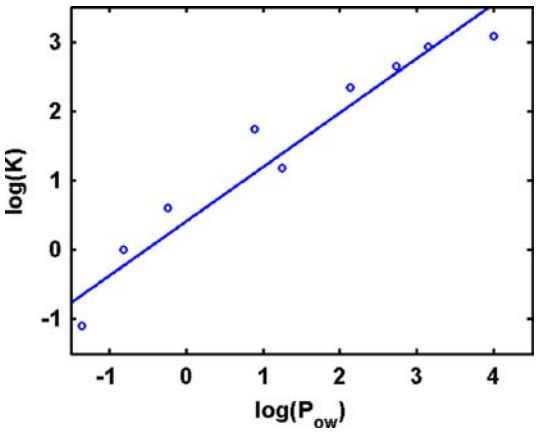

Fig. 4. Measured Teflon-water partition coefficients (K) vs. octanol-water partition coefficients (P_{ow}). The film's sensitivity increases with analyte hydrophobicity as characterized by P_{ow}. There is an approximate linear dependence between the log of each partition coefficient, which provides a general method for predicting interference from other contaminants.

For the range of BTX concentrations tested, film plasticization was not observed, as indicated by the film's linear response. The linear concentration dependence over the range of values tested is consistent with prior BTX vapor sensing results where Teflon films were found to exhibit a linear response to toluene vapor at concentrations up to 3549 ppm [15]. This vapor concentration would produce approximately the same degree of film saturation as toluene dissolved in water at 63 ppm, given the 53-fold difference in partitioning calculated from the measured film vapor and aqueous film sensitivities of 1.34×10^{-6} RIU/ppm and 7.1×10^{-5} RIU/ppm, respectively. We anticipate that the presence fluorocarbons [16] or hydrocarbons at higher concentrations [12] could plasticize the films, leading to changes in both the diffusion and partition coefficients of BTX solutes. The method of film preparation [15] may also affect these parameters. However, under such conditions, the film's refractive index would still increase although its sensitivity may be altered.

4. Conclusions

While the proposed Teflon-film refractive index-based sensing mechanism does not exhibit the same level of specificity as either absorption [27] or mass spectrometry based methods [6], it could readily be used for exclusionary testing of toluene or xylene, as the established limits of detection are well below the EPA maximum allowable levels [28] of 1 ppm for toluene and 10 ppm for xylene. While the measured LOD for benzene (183 ppb) is above the EPA maximum of 5 ppb, other SPR systems are capable of reducing the LOD to below 5 ppb. For instance, an SPR device [29] with a refractive index resolution of 1.8×10^{-7} would be capable of detecting benzene at a concentration of just 4.4 ppb, assuming the measured film sensitivity of 4.1×10^{-5} RIU/ppm. For a 3 μm film, the 63% equilibrium time is reached in approximately 5 min for benzene, demonstrating the possibility of rapid exclusionary testing. While the film's lack of specificity is a drawback, its high sensitivity to a broad range of hydrophobic contaminants may be advantageous for simultaneous screening of multiple potential hydrophobic contaminants, including polychlorinated biphenyl compounds [30]. A key advantage is that plasma-etched Teflon AF films may be used to functionalize any refractive index-based sensor for rapid exclusionary testing with no sample preparation.

References

[1] M. Smith, Ann. Rev. of Public Health 31 (2010) 133–148.
[2] V. Benignus, Neurotoxicology 2 (3) (1981) 567–588.
[3] F Gamberale, G. Annwall, M. Hultengren, J. Scandinavian, Work Environ. Health (1978) 204–211.
[4] Dominic C. DiGiuli, Investigation of Ground Water Contamination near Pavillion, Wyoming, Environmental Protection Agency, Washington DC, 2011.
[5] Benzene from gas plant leak polluting water near Parachute Creek, Denver Post, March 28, 2013.
[6] A. Monica, L. Cerdan, A. Godayol, E. Anticó, J. Sanchez, J. Chromatogr. A 1218 (45) (2011) 8131–8139.
[7] N. Rakhi, K. Reddy, M Saxena, R. Gupta, M Gupta, Elec. Dev., IEEE Trans 59 (10) (2012) 2809–2817.
[8] T. Erickson, K. Lear, IEEE Sens. J. 13 (5) (2013) 1905–1913.
[9] H. Zhang, S Weber, Fluorous Chem. (2012) 307–337.
[10] A. Polyakov, L. Starannikova, Y. Yampolskii, J. Membr. Sci. 216 (1) (2003) 241–256.
[11] F. Rupp, D. Axmann, C. Ziegler, J. Geis-Gerstorfer, J. Biomed. Mat. Res 62 (4) (2002) 567–578.
[12] I. Pinnau, L. Toy, J. Membr. Sci. 109 (1) (1996) 125–133.
[13] J. Rubio, J Arsuaga, M. Taravillo, V. Baonza, M. Cáceres, Exp. Therm Fluid Sci. 28 (8) (2004) 887–891.
[14] J. Sangster, J. Phys. Chem. Ref. Data 18 (3) (1989) 1111–1227.
[15] R. Podgorsek, H. Franke, Appl. Opt. 41 (4) (2002) 601–608.
[16] H. Zhang, S. Wang, S. Weber, Anal. Chem. 84 (22) (2012) 9920–9927.
[17] J. Edwards, D. Campbell J. Moore Integrated Optic Chemical Sensor for Environmental Monitoring, Photonics East (ISAM, VVDC, IEMB), Int. Soc. for Optics and Photonics (2009).
[18] B. Nelson, A. Frutos, J. Brockman, R. Corn, Anal. Chem. 71 (18) (1999) 3928–3934.
[19] J. Shiu, W. Whang, P Chen., J. Adhes. Sci. Technol. 22 (15) (2008) 1883–1891.
[20] W. Yunusand, A. Rahman, Appl. Opt. 27 (16) (1988) 3341–3343.
[21] J. Rim, P. Pinsky, W. van Osdol, Ann. Biomed. Eng. 33 (10) (2005) 1422–1438.
[22] J. Crank, The Mathematics of Diffusion, Eq. 2.67, Oxford University Press, 1975.
[23] R. Olmon, B. Slovick, T. Johnson, D Shelton, S. Oh, G. Boreman, M. Raschke, Phys. Rev. B: Condens. Matter 86 (23) (2012) 235147.
[24] O. Wolfbeis, J. Homola, Surface Plasmon Resonance Based Sensors, Springer-Verlag, Berlin-Heidelberg-New York, 2006.
[25] M. Born, E. Wolf, Principles of Optics, Pergamon, London, 1980.
[26] G. Long, J. Winefordner, Anal. Chem 55 (7) (1983) 712A–724A.
[27] M. Karlowatz, M. Kraft, B. Mizaikoff, Anal. Chem. 76 (9) (2004) 2643–2648.
[28] Edition of Drinking Water Standards, Office of Water, Environmental Protection Agency, Washington DC, 2012.
[29] T. Chinowsky, J. Quinn, D. Bartholomew, R. Kaiser, J. Elkind, Sensors and Actuators B 91 (1) (2003) 266–274.
[30] W. Shiu, D. Mackay, J. Phys. Chem. Ref. Data 10 (4) (1986) 1175–1199.